Reaction Kinetics, Mechanisms and Catalysis (2022) 135:3303–3315
https://doi.org/10.1007/s11144-022-02299-3

Green synthesis of silver nanoparticles using *Lathyrus brachypterus* extract for efficient catalytic reduction of methylene blue, methyl orange, methyl red and investigation of a kinetic model

Muradiye Şahin[1] · Yasin Arslan[2] · Fatma Tomul[3] · Bekir Yıldırım[4] · Hasan Genç[5]

Received: 21 May 2022 / Accepted: 5 September 2022 / Published online: 12 September 2022

Abstract

A facile, green, and an efficient method for the synthesis of AgNPs (silver nanoparticles) using *Lathyrus brachypterus* var. *brachypterus* extract is reported. AgNPs was characterized by UV–Vis, XRD, TEM and FTIR. The UV–Vis spectra of the AgNPs revealed a characteristic surface plasmon resonance peak at 452 nm. The synthesized AgNPs reacted as a heterogeneous catalyst for the reduction of dyes (methylene blue, methyl red and methyl orange) both in unary and ternary mixture (TM) with and without $NaBH_4$ (sodium borohydride). The kinetic parameter (k) for the degradation reactions and half-life ($t_{1/2}$) of dyes has been calculated according to Michaelis–Menten kinetics. Green synthesized of AgNPs effectively degraded the dyes at approximately 4–6 min. In addition, oxidation studies of methyl orange with H_2O_2 (hydrogen peroxide) have been also carried out and it has been reported that AgNPs can be reused as heterogeneous catalysts. The oxidation of MO was monitored with a UV–Vis spectrometer. AgNPs was separated using a filter paper after the oxidation of MO. The separated AgNPs were reused without important loss of its activity with a conversion efficiency of around 98%.

✉ Yasin Arslan
yasinarslan@mehmetakif.edu.tr

[1] Kırşehir Ahi Evran University, Campus, 40100 Kırşehir, Turkey

[2] Faculty of Arts and Science, Nanoscience and Nanotechnology Department, Burdur Mehmet Akif Ersoy University, Burdur, Turkey

[3] Faculty of Arts and Science, Chemistry Department, Burdur Mehmet Akif Ersoy University, Burdur, Turkey

[4] Burdur Food, Agriculture and Livestock Vocational School of Higher Education, Plant and Animal Production Department, Burdur Mehmet Akif Ersoy University, Burdur, Turkey

[5] Faculty of Education, Science Education Department, Burdur Mehmet Akif Ersoy University, Burdur, Turkey

Graphical abstract

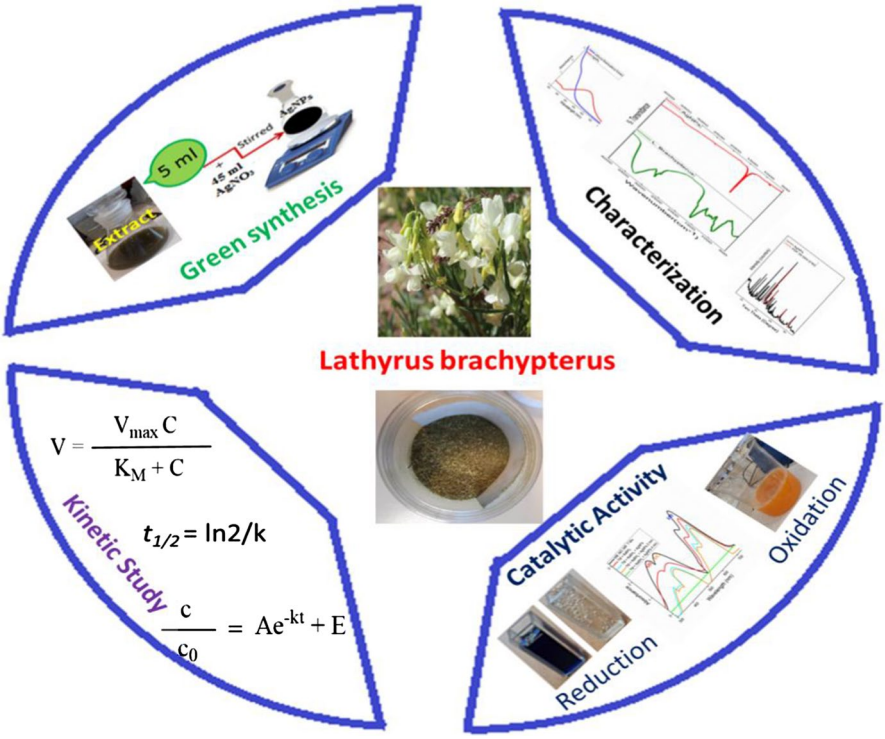

Keywords Catalytic activity · Dyes · Green synthesis · Lathyrus brachypterus · Oxidation

Introduction

In recent years, the silver nanoparticles (AgNPs) have been fascinated by the research community due to their large surface area, low melting point, catalytic, optical, sensor, pharmaceutical and biomedical properties [1–5]. The AgNPs can be prepared by various chemical and physical approaches, but chemical method is toxic and harmful to the environment [6]. This enables the researchers to turn for green approach, an eco-friendly and facile towards the synthesis of nanoparticles [7]. Various microorganisms, such as fungi and bacteria and various plant parts, such as fruit, seed, leaf, root and flower were successfully utilized for the synthesis of AgNPs [8–11]. In this present study, we propose a new endemic plant (*Lathyrus brachypterus*) which has safe, ecofriendly and non-toxic properties used as reduction and stabilizing agent for the synthesis of AgNPs. *Lathyrus* L. is a genus of plants with more than 200 taxa in the world [12]. 79 taxa, 25 of which are endemic, are distributed in the flora of Turkey [13–21]. Some species of the

genus are also used as human food or animal feed [22, 23]. *Lathyrus brachypterus* Čel., which was first defined by L. Čelakovský is a species belonging to this genus [24]. This species was later reduced to variety level as *L. brachypterus* var. *brachypterus*. *L. brachypterus* var. *haussknechtii* (Širj.) Davis, *L. pallescens* (Bieb.) Koch and *L. karsianus* P. H. Davis are the closest taxa taxonomically to mentioned taxon located in the Sect. *Platystylis*. The taxon distributed in Ankara, Kayseri, Adana, Kahramanmaraş, Niğde and Hatay provinces in Turkey is distinguished from its closest relative, *L. brachypterus* var. *haussknechtii*, by the pinnate leaves [13]. The morphological characteristics of *L. brachypterus* var. *brachypterus*, an endemic plant that grows on pastures and rocky slopes, are stated in Davis as follows: Plant erect, glabrous to ± pubescent, perennial. Stems wingless, 20–40 cm. median leaves pinnate or subdigitate, aristate; leaflets 2–3 paired, linear to oblong-linear, 25–55 × (1 −)2–7 mm, (3 −)5(−7) parallel-nerved, stipules lanceolate-subulate, longer than the 2–4 mm petiole. Peduncles 1–2 × leaves, rather closely 2–10 flowered. Flowers cream or pale sulphur, (15 −)18–25 mm. Calyx (5 −)6–9 mm; teeth unequal, the lowest slightly shorter than tube. Style filiform except for the slightly dilated apex, (6.5 −)7–10 × 0.5–1 mm. Legumes (immature) linear. In the current study, the ability of this taxon to synthesize AgNPs was tested and it was observed that AgNPs were successfully synthesized with a high yield.

The release of organic dye effluents from textile, leather, cosmetic, paper, food and plastic industries pollute the environment because of the recalcitrance, undesirability and high visibility of these dye stuffs [25, 26]. During different dyeing processes in the textile industry, approximately 200 billion liters of colored wastewater are produced annually, depending on the type of fabric and dye, and this wastewater pollutes the both surface and groundwater, posing a danger to aquatic life, humans and the environment [27, 28]. In general, dyes particularly affect aquatic organisms [29] and they cause eutrophication and reduce the oxygen capacity of the water, preventing the penetration of sunlight [29]. In addition, many of these dyes are mutagenic and carcinogenic [30]. Therefore, it is essential to develop environmentally friendly and inexpensive methods to eliminate these dyes contamination from the environment.

The aim of this study is to use AgNPs synthesized by green method to remove some dangerous dyes from water solution because unloading of these dangerous dyes from textile industries in the groundwater, rivers and lakes has become an earnest problem, which contributes to boost their pollution levels severely. These pollutants are difficult to eliminate by traditional water treatment procedures. In this study, three type dyes, such as a thiazine dye (methylene blue, MB) and azo dyes (methyl red, MR and methyl orange, MO) with different chemical structures have been chosen to evaluate the catalytic performance of synthesized AgNPs. Degradation rate of dyes both in unary and ternary mixture (TM) was occurred as nearly 100% within between 4 and 6 min. Finally, it has been proved that green synthesized AgNPs have efficient catalytic activity for comprehensive reduction and oxidation of organic dye compounds with high efficiency. Furthermore, AgNPs have been successfully reused without lossing of their catalytic activities.

Material and methods

Materials

Silver nitrate ($AgNO_3$) and sodium borohydride ($NaBH_4$) were obtained from Fluka. Hydrogen peroxide (H_2O_2) and MB were obtained from Sigma-Aldrich. MO and MR were obtained from Merck. All solutions in experimental studies were prepared with high purity water (18 MΩ cm) obtained from PURIS pure water system (PURIS, Expe-UP Series). All of the materials were in analytical reagent grade and utilized as received without any purification.

Instrumentation

The chemical and morphological characterizations for the synthesized AgNPs were performed by Shimadzu UV-1800 (UV–Vis), Perkin Elmer Fronter model FT-IR, Bruker D8 Advance model X-ray diffraction (XRD) with a CuKa radiation source in 2θ range from 10° to 90°, TEM-120 kV Transmission Electron Microscope (TEM).

Synthesis of AgNPs

1.0 g of *Lathyrus brachypterus* was gauged and mixed with 50 mL of distilled water. The mixture was stirred continuously at 25 °C for 5 h and solid phase was separated with a filter paper to obtain *L. brachypterus* extract [5, 25]. To prepare AgNPs, 5 mL of extract was mixed with 0.1 M, 45 mL of $AgNO_3$. Then, the mixture was left at room temperature with magnetic stirrer to efficiently complete the synthesis of AgNPs in which plant extract acted as both stabilizer and reductant. After the reduction of Ag^+ ions to Ag^0 was completed for about 5–6 min, the AgNPs were filtered through a Whatman No 1 filter paper (90 mm, 82 g/m^2 and pore size: 15–19 µm). The synthesis of AgNPs was also recognized by both the color change of mixture and the characteristic resonance band observed by UV–Vis spectrum (Fig. 1). As a result, 625 mg AgNPs was synthesized in

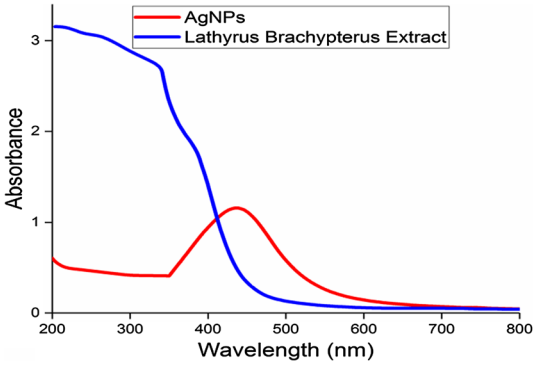

Fig. 1 UV–Vis spectra of the *L. brachypterus* extract and AgNPs (nanoparticle preparation conditions: plant extract volume 5 mL, $AgNO_3$ concentration 0.1 M and room temperature)

relatively high yield (85.71%) in an environmentally friendly method using the endemic plant extract of lathyrus brachypterus powder at room temperature without using any reducing chemicals.

Catalytic activity of AgNPs

The catalytic activity of AgNPs was investigated using the degradation of some dyes such as MR, MB and MO using both with $NaBH_4$ and without $NaBH_4$. These three dyes are chosen due to the exhibition distinct colours for both reduced and oxidized structures. The reduction of these dyes both in unary and TM in the existence with both AgNPs and/or $NaBH_4$ was conducted at 25 °C. For this, 1 mL of $NaBH_4$ (1×10^{-2} mol L^{-1}) was mixed with 1 mL of dyes (1×10^{-3} mg L^{-1}). Then, 0.5 mL (14 mg) AgNPs was added to this mixture and the UV–Vis spectra were used at regular intervals to follow the reduction of dyes which were shown by the decolorization of the solution to colorless. The concentrations of MR, MO and MB dyes were quantified by measuring the absorption band at 415, 460 and 664 nm [31, 32].

These dyes and their degradation products are:

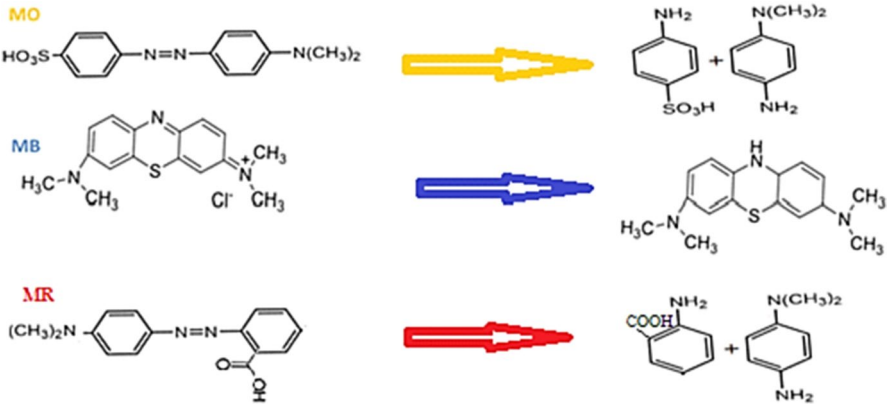

In addition, the catalytic activity of AgNPs was also investigated with the oxidation degradation studies for the MO dye. The oxidation of MO with AgNPs used as heterogeneous catalyst in the presence of H_2O_2 was carried out at room temperature. For this, 0.1 g AgNPs catalyst was added to 100 mL of 25 ppm MO solution. Then, 3 mL of 30% H_2O_2 was added and mixed at 300 rpm (pH = 6.80) in a magnetic stirrer at room temperature. By taking 3 mL of the mixture at regular intervals, UV–Vis measurements were performed. It was observed that the oxidation was completed after the color removal of the dye and with the disappearance of the MO peak (pH = 5.2). After oxidation, the mixture was centrifuged at 7000 rpm for 3 min and AgNPs were separated from the mixture by filtration, and 3 cycles of measurements were performed to test the reusability of AgNPs.

Results and discussion

Characterization

The AgNPs were characterized by FTIR, UV–Vis, HR-TEM (high resolution-TEM) and XRD. The UV − Vis spectroscopy is a generally used to determine the different metal nanoparticles [33]. The synthesis of AgNPs using endemic plant extract was firstly decided with the colour changes in which a light green colour of solution was gradually changed to black colour. In addition, in the UV–Vis spectral analysis, the characteristic absorbance peak at about 452 nm is commonly used for the definition of AgNPs [5, 26, 34, 35]. UV–Vis spectra of both plant extract and AgNPs were given in Fig. 1.

In order to support the synthesis of AgNPs and to understand on which bonds the nanoparticle proceeds, FT-IR analyzes of both plant extract and AgNPs were performed and given in Fig. S1 as comparatively. In the FT-IR spectra of plant extract, –OH peak was observed at 3285 cm^{-1}. The peak observed at 2973 cm^{-1} corresponds to N–H bond, the peak observed at 1650 cm^{-1} corresponds to C = C double bonds or aromatic rings, and the peak observed at 1420 cm^{-1} corresponds to C = O stretching in the carboxyl group. The peak observed at 1026 cm^{-1} corresponds to the stretching of the amines—CN—and the peak observed at 602 cm^{-1} corresponds to the C–H vibration. The peak observed at 1307 cm^{-1} may be associated with geminal methyl. FT-IR results prove the presence of alkaline, methylene, alkene, amine, phenol and carboxyl groups in the plant extract. These chemical groups have proven to be reducing agents that assist in the synthesis of AgNPs [34, 35]. When FTIR spectra of the both plant extract and AgNPs are compared, it is seen that the peak intensities are either very weak or completely lost in the AgNPs spectra with respect to the plant extract spectra suggesting that the endemic plant used for the first time, is an effective reducing agent for the synthesis of AgNPs.

In order to determine the crystal structure of the synthesized AgNPs, XRD analysis was performed and the XRD measurement result was given in Fig. S2. As a result of the obtained diffraction patterns, peaks belonging to (111), (200), (220) and (311) crystal structures were observed corresponding to the angle values of 2θ = 38.1°, 44.3°, 64.4° and 77.5° for metallic silver (JCPDS 04-0783). From these results, it was understood that there was a metallic silver in a face-centered cubic structure. In addition, it was concluded from the diffraction patterns that the metals from the plant were found as impurities. In this part of study, particle sizes of AgNPs were calculated using the Scherrer equation from the XRD results.

Calculation of D_{111} particle size using the Scherrer equation;

$$D_{111} = \frac{k\lambda}{(\beta \cos\theta)} \tag{1}$$

Here D_{111} is the particle size (nanometers), k = 0.94 is the constant associated with the crystal shape, β is the measure of the full width of half hight of the peak at the maximum intensity (in the 111 plane) in the spectrum, ʎ is the X-ray wavelength, and θ is the angle of the diffraction peak (Bragg). The average particle size of

AgNPs found in the calculation with the characteristic Ag (111) peak was found to be 6.08 nm.

TEM analyzes were also performed to observe the geometric properties, particle size and distribution of the synthesized AgNPs. It is observed in Fig. S3 that AgNPs are formed properly, they are in crystalline structure and there is no big difference between their sizes. In addition, from the size distribution histogram in Fig. S3, it is seen that the nanoparticle size varies between 6 and 30 nm; the average size of the particles was found to be 14.15 ± 0.20 nm. As seen, there is a good agreement with the particle sizes calculated by the Scherrer equation in the XRD spectra shown in Fig. S2.

Catalytic activity

The catalytic activity of AgNPs for MR, MO and MB dyes in both unary and TM were investigated at 25 °C. This process was described in section "Catalytic activity of AgNPs". These dyes and their degradation products were also given in section "Catalytic activity of AgNPs". For the removal of these dyes, AgNPs and/or $NaBH_4$ were used. Firstly the experiments were carried out only using $NaBH_4$. For this, 1 mL of dyes was taken in quartz cuvettes and then 1 mL of $NaBH_4$ (1×10^{-2} mol L^{-1}) solution was added to this dye solution. Initially, there was a slightly color change occurred in the dyes but then $NaBH_4$ could not further reduce the dye even after 1–2 h. The experimental results reveal that only $NaBH_4$ is not so effective for completely reducing the dyes and AgNPs are needed to completely reduce the dye compounds to their degradation products. Moreover, it was also observed from the experimental results that all dyes were successfully adsorbed in a short time with only using AgNPs synthesized by using endemic plant extract without needing any chemicals because of their strong adsorption property (Figs. S4-S7).

For the degradation mechanism, it can be said that BH_4^- ions formed by $NaBH_4$ ionization diffuse into AgNPs together with dye molecules. These emitted BH_4^- ions produce bonded hydrogen on the AgNPs surface. The dye molecules reach onto the AgNPs surface and are quickly bound there due to electrostatic interactions (due to negative charge on the Ag surface and positively charged dye molecules). The hydrogen interacts with the dye molecules through the nanoparticle, which acts as an electron carrier, and the dye molecules are then degraded. In addition, while BH_4^- ions are nucleophilic, dye molecules are electrophilic compared to metal nanoparticles. During the catalytic decomposition reaction, dye molecules capture electrons from BH_4^- ions via metal nanoparticles. Thus, metal nanoparticles play a role as electron transfer center in dye degradation in the presence of $NaBH_4$. It has been accepted that the possible reduction reaction mechanism of dyes occurs through the following steps [36].

$$\mathrm{Ag/NaBH_4} + h\surd \rightarrow \mathrm{Ag/NaBH_4(h^+ - e^-)}$$

$$2e + \mathrm{MOH^+} + \mathrm{H^+} \rightarrow \mathrm{MOH_2(Degradation\ product)}$$

In addition to adsorption and/or degradation of dyes by AgNPs, the oxidation of MO at room temperature was also performed as described in section "Catalytic activity of

AgNPs". For the reusability of AgNPs heterogeneous catalysts, 3 cycles of measurements were made; they have been observed that they can be successfully reused without significant loss in their catalytic activities (Fig. 2).

In principle, it can be said that the decompositions of dyes by oxidation are based on the principle of producing OH· radicals. H_2O_2 adsorbed by the metal nanoparticle takes electrons from the metal nanoparticle and forms OH· radicals as a result of OH^- ion oxidation. These radicals adsorbed by the nanoparticle react with the dye on the surface and cause the dyes to decompose. In other words, the OH· radical oxidizes the dye and converts it to CO_2 and H_2O. The rate of catalytic oxidation depends on both adsorptions of H_2O_2 on the nanoparticle surface and electron transfer from the nanoparticle. It can be said that nanoparticles effectively weaken the O–O bond, providing an advantage for H_2O_2 adsorption and increasing the electron transport rate. In the literature, it has been explained that the possible oxidation reaction mechanism of MO occurs in the presence of hydroxyl (HO·) and hydroperoxyl (HOO·) radicals formed from H_2O_2 [37].

Kinetic study

The process of catalytic degradation of MB, MR and MO dyes both in unary and TM were found to follow the pseudo-first-order kinetic model.

$$-\frac{dc_t}{dt} = kc \tag{2}$$

$$\frac{c}{c_0} = Ae^{-kt} + E \tag{3}$$

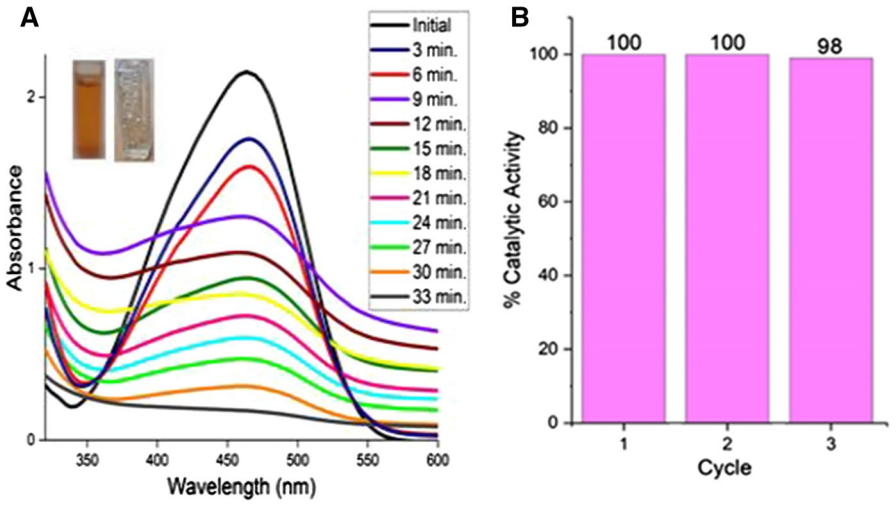

Fig. 2 **A** UV–Vis spectra of degradation of MO dye using AgNPs catalyst. (3 mL; Concentration of mixture MO; 25 ppm 100 mL, H_2O_2; %30 3 mL, nanoparticle; 0.1 g) **B** Reusability of AgNPs

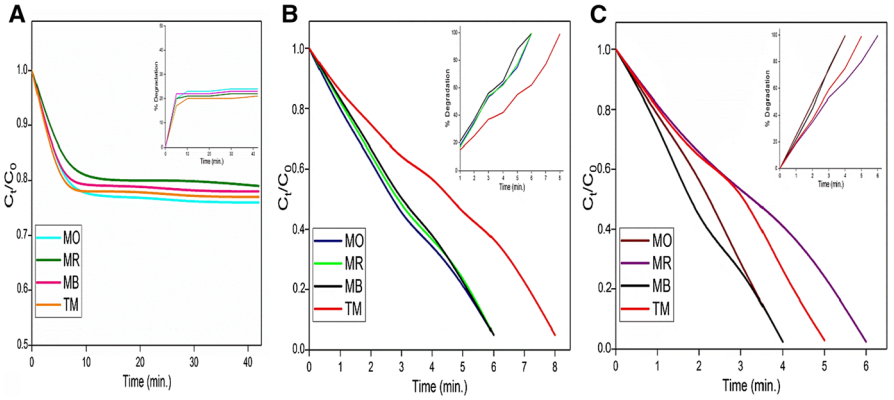

Fig. 3 % Reduction of dyes and Pseudo-first order kinetic model for degradation of MB, MR, MO dyes both in unary and TM using **A** only $NaBH_4$ **B** only AgNPs **C** AgNPs with $NaBH_4$ (Concentration of dye; 1 mL, 1×10^{-3} mg L^{-1}, $NaBH_4$; 1 mL 1×10^{-2} mol L^{-1}, nanoparticle solution with water; 0.5 mL)

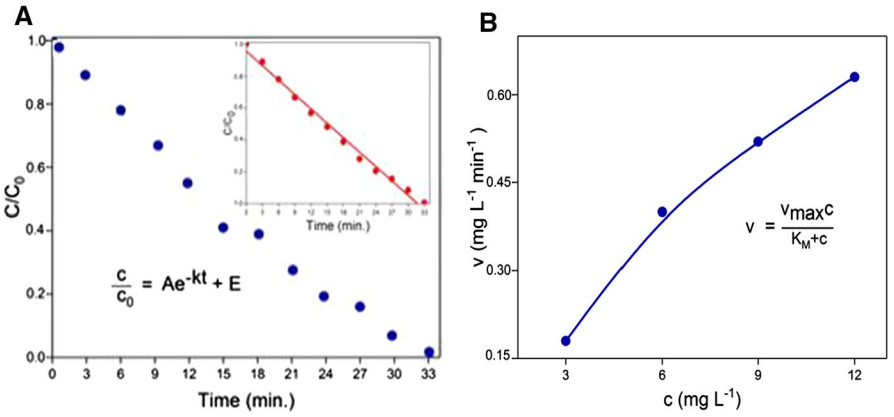

Fig.4 **a** Pseudo-first order kinetic model for oxidation of MO, **b** The curves of the Michaelis–Menten kinetics of the degradation of MO by AgNPs. The above curves were obtained by non-linear least squares fitting. (3 mL, concentration of mixture MO; 25 ppm 100 mL, H_2O_2; %30 3 mL, nanoparticle; 0.1 g)

Here, C and C_0 are dyes concentrations at t time interval and initial, respectively. k is the reaction rate constant; t is the reaction time. The values of rate constant and standard deviations are obtained by non-linear least squares fitting [38, 39], as shown in Figs. 3, 4a and Table 1.

$$t_{1/2} = \ln 2/k \tag{4}$$

Equation 4 can be used to calculate the half-life $t_{1/2}$ of dyes with AgNPs and all results are listed in Table 1. Moreover, the catalytic degradation is calculated

Table 1 The kinetic data results

	Dye	k (min^{-1})	R^2	$t_{1/2}$ (min)
$AgNPs + NaBH_4$	MB	0.3014 ± 0.0005	0.9915	2.3
	MO	0.3301 ± 0.0001	0.9999	2.1
	MR	0.2166 ± 0.0010	0.9857	3.2
	TM	0.2888 ± 0.0008	0.9892	2.4
Only AgNPs	MB	0.2100 ± 0.0013	0.9850	3.3
	MO	0.2236 ± 0.0009	0.9864	3.1
	MR	0.2166 ± 0.0010	0.9857	3.2
	TM	0.1733 ± 0.0017	0.9801	4.0
$AgNPs + H_2O_2$	MO	0.0420 ± 0.0021	0.9727	16.5

according to Michaelis–Menten kinetics [39] and the effect of the initial concentration on the MO oxidation rate is found by the Eq. 5.

$$V = \frac{V_{max} C}{K_M + C} \tag{5}$$

Here, V is the initial rate, C represents concentration, V_{max} and K_M are related to maximum initial rate and Michaelis constant, respectively. When the initial concentration range of MO is 3–12 mg L^{-1}, the values of V_{max} and K_M can be obtained by non-linear least squares fitting [40]. Fig. 4b depicts that the dyes concentration ranges in Michaelis–Menten curve is suitable. V_{max} and K_M are calculated as 0.6614 ± 0.0099 mg L^{-1} min^{-1} and 1.2056 ± 0.2800 mg L^{-1}, respectively.

Conclusion

AgNPs were easily, reliably, economically synthesized with high yield (85.71%) by endemic lathyrus brachypterus plant extract used for the first time for the synthesis of AgNPs. Based on UV–Vis, FT-IR, XRD and TEM characterization results, AgNPs were successfully synthesized and it was observed in the FTIR spectra that the carboxyl, amine and phenol groups found in the endemic plant extract were effective for both reduction and stabilization. In addition, it was observed from XRD spectra that the synthesized AgNPs were in a face-centered cubic crystalline structure and the average particle size of AgNPs using the characteristic Ag (111) peak is found to be 6.08 nm. Based on TEM results, the nanoparticle sizes were varied between 6 and 30 nm and they were consistent with XRD results. Furthermore, the catalytic activities of synthesized AgNPs used as heterogeneous catalysts were investigated for the removing of MB, MO and MR dyes and their kinetic parameters were calculated. For this, the degradation studies of MB, MO and MR dyes were carried out using only $NaBH_4$, only AgNPs and AgNPs in the presence with $NaBH_4$ for both in unary and TM. As a result of the catalysis applications, all dyes were reduced in a very short time between 4 and 6 min with AgNPs in the presence with $NaBH_4$. It was also observed that when only $NaBH_4$ was used, the reduction process

was not efficiently occurred and only 20% of dyes were reduced in a period of 1 h. On the other hand, AgNPs alone were effective for the adsorption of dyes in a short period of time between 6 and 8 min. In addition, the synthesized AgNPs were used as a heterogeneous catalyst in the oxidation decomposition studies of the MO dye in the presence with H_2O_2. It was observed in this study that the dye was degraded in a shorter time than the times given in the literature. The reusability of AgNPs was also tested by performing 3 more cycles of oxidation study and a conversion efficiency was found to be 98% without losing activity. The kinetic parameter (k) and half-lives ($t_{1/2}$) of the dyes for the degradation reactions of the dyes were calculated according to the Michaelis–Menten kinetics.

Supplementary Information The online version contains supplementary material available at https://doi.org/10.1007/s11144-022-02299-3.

References

1. Arumai SD, Mahendiran D, Senthil KR, Kalilur RA (2018) Garlic, green tea and turmeric extracts-mediated green synthesis of silver nanoparticles: phytochemical, antioxidant and in vitro cytotoxicity studies. J Photochem Photobiol B 180:243–252
2. Firdaus M, Andriana S, Elvinawati AW, Swistoro E, Ruyani A, Sundaryono A (2017) Green synthesis of silver nanoparticles using *Carica papaya* fruit extract under sunlight irradiation and their colorimetric detection of mercury ions. J Phys: Conf Ser 817:012029
3. Selvapriya V, Deepa C (2017) A novel, comparative study of chemical and green synthesis of silver nanoparticles. J Environ Nanotechnol 6(1):23–26
4. Skiba MI, Vorobyova VI, Pivovarov A, Makarshenko NP (2020) Green synthesis of silver nanoparticles in the presence of polysaccharide: optimization and characterization. J Nanomater 3051308:1–10
5. Sahin M, Gubbuk IH (2019) Green synthesis of antioxidant silver and platinum nanoparticles using ginger and turmeric extracts and investigation of their catalytic activity. J Turkish Chem Soc A 6(3):403–410
6. Vijayaraghavan K, Ashokkumar T (2017) Plant-mediated biosynthesis of metallic nanoparticles: a review of literature, factors affecting synthesis, characterization techniques and applications. J Environ Chem Eng 5:4866–4883
7. Bindhu MR, Umadevi M, Esmail GA, Al-Dhabi NA, Arasu MV (2020) Green synthesis and characterization of silver nanoparticles from *Moringa oleifera* flower and assessment of antimicrobial and sensing properties. J Photochem Photobiol B 205:111836
8. Sherin L, Sohail A, UeS A, Mustafa M, Jabeen R, Ul- Hamid A (2020) Facile green synthesis of silver sanoparticles using terminalia bellerica kernel extract for catalytic reduction of anthropogenic water pollutants. Colloids Interface Sci 37:100276
9. Bernardo-Mazariegos E, Valdez-Salas B, Gonzalez-Mendoza D, Abdelmoteleb A, Camacho OT, Duran CC, Gutierrez-Micelic F (2019) Silver nanoparticles from justicia spicigera and their antimicrobial potentialities in the biocontrol of foodborne bacteria and phytopathogenic fungi. Rev Argent Microbiol 51:103–109
10. Devi LS, Joshi SR (2012) Antimicrobial and synergistic effects of silver nanoparticles synthesized using soil fungi of high altitudes of eastern himalaya. Mycobiology 40:27–34
11. Pawar JS, Patil RH (2020) Green synthesis of silver nanoparticles using *Eulophia herbacea* (lindl.) tuber extract and evaluation of its biological and catalytic activity. SN Appl Sci 2:52
12. Allkin R, Goyder DJ, Bisby FA, White RJ (1986) Names and synonyms of species and subspecies in the Vicieae. Issue 3. Vicieae database project. University of Southampton, Southampton, UK
13. Davis PH (1970) In: Davis PH (Ed) Flora of Turkey and the East Aegean Islands, Vol. 3. Edinburgh University Press, Edinburgh, 328–369.
14. Davis PH, Mill RR, Tan K (Eds) (1988) Flora of Turkey and the East Aegean Islands, Vol. 10 (Supplement), Edinburgh University Press, Edinburgh, 125–126.

15. Güneş F, Özhatay N (2000) In: Güner A, Özhatay N, Ekim T, Başer KHC (Eds), Flora of Turkey and the East Aegean Islands, Vol. 11 (Supplement 2), Edinburgh University Press, Edinburgh, 92-94.
16. Genç H (2009) *Lathyrus nivalis* subsp. sahinii subsp. nov. (Sect. Platystylis, Leguminosae) from Turkey. Nord J Bot 27:402–404
17. Genç H, Şahin A (2008) A new species of *Lathyrus* L. (section Cicercula; Fabaceae) from Turkey. Bot J Linn Soc 158:301–305
18. Genç H, Şahin A (2011) A new species of *Lathyrus* L. (Fabaceae) from Turkey. J Syst Evol 49(5):505–508
19. Güneş F, Çırpıcı AH (2012) A new record for the of Turkey: *Lathyrus atropatanus* (Leguminosae). Turk J Bot 36:425
20. Güneş F (2014) A new species of *Lathyrus* (Fabaceae) from Turkey. Pensee J 76(3):339–350
21. Güneş F (2018) Türkiye florası için yeni bir mürdümük [Lathyrus pannonicus (Jacq.) Garcke subsp. collinus (Ortmann) Soó (Fabaceae)] kaydı. Bağbahçe Bilim Derg 5(2): 1–9
22. Yamamoto K, Fujiwara T, Blumenreich I (1984) Karyotypes and morphological characteristics of some species in the *Lathyrus* L. Jpn J Breed 34:273–284
23. Genç H, Şahin A (2001) Batı Akdeniz ve Güney Ege Bölgesinde yetişen Bazı Lathyrus L. türleri üzerinde sitotaksonomik araştırmalar III. S.D.Ü. Fen Bilimleri Dergisi 5(1): 98–112.
24. Čelakovský L (1888) Ueber einige neue orientalische pflanzenarten. Oesterreichische botanische zeitschrift 38:44–48
25. Sahin M, Gubbuk IH (2022) Green synthesis of palladium nanoparticles and investigation of their catalytic activity for methylene blue, methyl orange and rhodamine B degradation by sodium borohydride. React Kinet Mech Catal 135:999–1010
26. Trak D, Arslan Y (2021) Synthesis of silver nanoparticles using dried black mulberry (*Morus nigra* L.) fruit extract and their antibacterial and effective dye degradation activities. Inorg Nano-metal Chem. https://doi.org/10.1080/24701556.2021.1980038
27. Varadavenkatesan T, Selvaraj R, Vinayagam R (2020) Green synthesis of silver nanoparticles using thunbergia grandiflora flower extract and its catalytic action in reduction of congo red dye. Materialstoday Proc 23(1):39–42
28. Tripathi RM, Shrivastav BR, Shrivastav A (2018) Antibacterial and catalytic activity of biogenic gold nanoparticles synthesised by trichoderma harzianum. IET Nanobiotechnol 12:509–513
29. Jaleh B, Karami S, Sajjadi M, Mohazzab BF, Azizian S, Nasrollahzadeh M, Varma RS (2020) Laser-assisted preparation of pd nanoparticles on carbon cloth for the degradation of environmental pollutants in aqueous medium. Chemosphere 246:125755
30. Suvarna AR, Shetty A, Anchan S, Kabeer N, Nayak S (2020) Cyclea peltata leaf mediated green synthesized bimetallic nanoparticles exhibits methyl green dye degradation capability. Bionanoscience 10:606–617
31. Garg N, Bera S, Rastogi L, Ballal A, Balaramakrishna MV (2020) Synthesis and characterization of L-asparagine stabilised gold nanoparticles: catalyst for degradation of organic dyes. Spectrochim Acta A Mol Biomol Spectrosc 232:118126
32. Bogireddy NKR, Kumar HAK, Mandal BK (2016) Biofabricated silver nanoparticles as green catalyst in the degradation of different textile dyes. J Environ Chem Eng 4:56–64
33. Baruwati B, Varma RS (2009) High value products from waste: grape pomace extract—a three-in-one package for the synthesis of metal nanoparticles. Chem Sus Chem 2(11):1041–1044
34. Baghayeri M, Mahdavi B, Abadi ZHM, Farhadi S (2018) Green synthesis of silver nanoparticles using water extract of *Salvia leriifolia*: antibacterial studies and applications as catalysts in the electrochemical detection of nitrite. Appl Organometal Chem 32:4057
35. Balwe SG, Shinde VV, Rokade AA, Park SS, Jeong YT (2017) Green synthesis and characterization of silver nanoparticles (Ag NPs) from extract of plant *Radix puerariae*: An efficient and recyclable catalyst for the construction of pyrimido[1,2-b]indazole derivatives under solvent-free conditions. Catal Commun 99:121–126
36. Vidhu VK, Philip D (2014) Catalytic degradation of organic dyes using biosynthesized silver nanoparticles. Micron 56:54–62
37. Han J, Zeng HY, Xu S, Chen CR, Liu XJ (2016) Catalytic properties of CuMgAlO catalyst and degradation mechanismin CWPO of methyl orange. Appl Catal A 527:72–80
38. Xu Q, Mavengere S, Kim JS (2021) Preparation of the $CaAl_2O_4$:Eu^{2+}, Nd^{3+}/TiO_2 composite by peroxo titanium complex solution and its photodegradation of methylene blue. React Kinet Mech Catal 134:473–484

39. Lente G (2018) Facts and alternative facts in chemical kinetics: remarks about the kinetic use of activities, termolecular processes, and linearization techniques. Curr Opin Chem Eng 21:76–83
40. Gholami P, Dinpazhoh L, Khataee A, Hassani A, Bhatnagar A (2020) Facile hydrothermal synthesis of novel Fe-Cu layered double hydroxide/biochar nanocomposite with enhanced sonocatalytic activity for degradation of cefazolin sodium. J Hazard Mater 381:120742